BULLETIN OF THE POLISH ACADEMY OF SCIENCES
TECHNICAL SCIENCES, Vol. 67, No. 6, 2019
DOI: 10.24425/bpasts.2019.131569

Fast optimal feedback controller for electric linear actuator used in spreading systems of road spreaders

D. DOBROWOLSKI[1], J. DOBROWOLSKI[1], W. PIEKARSKA[2], and S. STĘPIEŃ[3]*

[1] Dobrowolski LLC Company, Obrońców Warszawy 26A, 67-400 Wschowa, Poland
[2] Czestochowa University of Technology, Institute of Mechanics and Machine Design Foundations, Dąbrowskiego 73, Czestochowa, Poland
[3] Poznan University of Technology, Institute of Automation and Robotics, Piotrowo 3a, 60-965 Poznan, Poland

Abstract. Modern and innovative road spreaders are now equipped with a special swiveling mechanism of the spreading disc. It allows for adjusting a symmetrical or asymmetrical spreading pattern and provides for the possibility to maintain the size of the spreading surface and achieve an accurately defined spreading pattern with spreading widths. Thus the paper presents a modelling and control design methodology, and the concept is proposed to design high-performance and optimal drive systems for spreading devices. The paper deals with a nonlinear model of an electric linear actuator and solution of the new intelligent/optimal control problem for the actuator.

Key words: linear electric actuator, nonlinear modelling, optimal feedback control.

1. Introduction

Replacing hydraulic or pneumatic cylinders with electrical linear actuators means a simpler and smaller-size installation, easier control, lower energy costs, higher accuracy, less maintenance, less noise and cleaner, healthier environment [3–5].

Electrical actuator systems ensure consistent operation in both directions. They also have additional features such as end-of-stroke limit switches, mid-stroke protection and manual override operation in case of a power failure. Optional features such as analog or digital position feedback and adjustable end-of-stroke limit switches are also available. Moreover, their vast advantage lies in that the system is easy to integrate with other control systems found in industrial systems such as PLCs, microcontrollers, computers or simple relay based systems [4, 5, 21].

Electric actuators are widely used in agriculture, construction, mining, forestry, road work and the railway equipment industry for the control of seats, hoods, doors, covers, balers, pantographs, sprayer booms, throttles and many more.

Positioning control of such actuation systems constitutes a significant research subject in both engineering and science [3]. In literature, there are many works related to modelling and control of linear electric actuators, especially in the fields where high-speed motion is required. Some design approaches are reported in [4]. However, there still exist numerous meaningful challenges, for example, controller designers are likely to encounter serious nonlinearities and disturbances which refer to nonlinear friction, nonlinear parasitic force or precise positioning with high speed [5].

This paper shows application of the high performance finite-time SDRE-based suboptimal control of an electric linear actuator mounted onto a spreading device system as part of road/highway spreaders [22].

The method, first proposed in 1962 [11] and later expanded in 1975 [6], was further studied in more detail, creating its final and useful form for practical implementation [8]. The method entails parameterization of the nonlinear dynamics into the state vector and the product of a matrix-valued function that depends on the state itself [12]. The control algorithm fully captures the nonlinearities of the system, bringing the nonlinear system to a (non-unique) linear structure having state-dependent coefficient (SDC) matrices, and minimizing a nonlinear performance index having a quadratic-like structure.

An algebraic Riccati equation (ARE), using the SDC matrices, is then solved on-line to give the suboptimum control law. The SDRE feedback scheme for the infinite-time nonlinear optimal control problem in the multivariable case is locally asymptotically stable and locally asymptotically optimal, as described in first solid theoretical contributions [1, 8, 10, 13, 18].

Applications of the SDRE control technique also include satellite and spacecraft control and estimation, integrated guidance and control design, autopilot design, robotics, control of systems with parasitic effects, control of artificial human pancreas, ducted fan control and magnetic systems, including levitation [1, 14].

Figure 1 shows the spreading vehicle for winter road service with the spreading device indicated as a control plant.

The spreading device for winter road service vehicles, used for applying spreading material, comprises a spreading material container, a dispersing unit and a spreading material conveyor section, arranged between the spreading material container and the dispersing unit. The dispersing unit contains a rotary spread-

*e-mail: Slawomir.Stepien@put.poznan.pl

Manuscript submitted 2019-04-25, revised 2019-06-30, initially accepted for publication 2019-08-01, published in December 2019

Fig. 1. Road spreading vehicle.

ing plate. The spreading material drops on the rotary plate via a metal claim. The claim can be positioned by the linear actuator to change spreading width or spreading range angle. This function is very important and useful, because:

- the spreading angle depends on the width of the road,
- the angle must be changed on-line employing a special control system for passing cars or other object protection.

The second function involves the swiveling mechanism of the spreading disc, which allows for adjusting a symmetrical or asymmetrical spreading pattern electronically via a special control system. Application of the SDRE technique to the finite time horizon control of a linear actuator mounted onto a spreading device system is a challenge because the control time depends on passing car speed. This technique makes it possible to maintain the size of the spreading surface and achieve an accurately defined spreading pattern with the spreading widths. The function is now implemented and introduced in modern and innovative spreading vehicles. Range angle control is realized by means of positioning of an electric linear actuator as shown in Fig. 2.

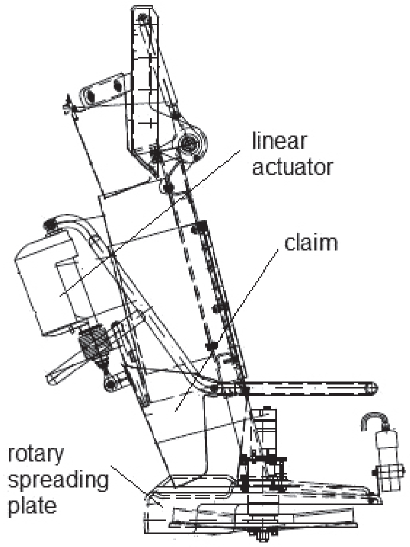

Fig. 2. Spreading subsystem.

In this paper, the modelling and control design methodology concept is proposed to design high-performance and optimal drive systems for spreading devices. The paper presents a nonlinear model of an electric linear actuator along with the solution of the finite-time suboptimal control problem for the actuator.

2. Actuator modelling

The linear actuator consists of a permanent magnet DC motor with an electromagnetic-force-actuated positioning system.

Fig. 3. Linear actuator.

The control plant is equipped with a gear and mechanical overload protection system through an integrated slip clutch. An integrated brake ensures high self-locking ability. The brake is deactivated when the actuator is powered in order to obtain high efficiency.

The actuator model is an electro-mechanical system. Thus, it should be described by equations of the mechanical motion and electric circuit system [4, 5].

The force equilibrium relationship in the motion system, considering dynamic friction, is given by:

$$M\ddot{x}(t) + F_{fric}(\dot{x}) = F(t) \tag{1}$$

where M is a moving mass and x denotes position. The force generated by an actuator is proportional to motor current i:

$$F(t) = k_f i(t). \tag{2}$$

The dynamic nonlinear friction via Stribeck model [3] is as follows:

$$F_{fric}(\dot{x}) = \left(F_c + (F_m - F_c)\, e^{-\alpha}\, |\dot{x}(t)|\right) sign(\dot{x}(t)) + \beta\dot{x}(t) \tag{3}$$

where F_m is maximum static friction, F_c is Coulomb friction, α is a damping coefficient which depends on servo system, and β denotes the coefficient of viscosity.

The electric circuit equation in the DC motor is described by the motor current, with consideration of winding resistance and inductance:

$$L\frac{\mathrm{d}i(t)}{\mathrm{d}t} + Ri(t) + k_e\dot{x} = u(t) \tag{4}$$

where L denotes inductance, R denotes resistance, the term $k_e\dot{\boldsymbol{x}}$ stands for back electromotive force and u is motor terminal voltage.

Employing the state-space modelling technique, the linear actuator model can be described by the nonlinear equation system as follows:

$$\frac{\mathrm{d}}{\mathrm{d}t}\begin{bmatrix} x_1 \\ x_2 \\ x_3 \end{bmatrix} = \begin{bmatrix} x_2 \\ -\frac{F_{cm}}{M} sign\,(x_2) - \frac{\beta}{M}x_2 + \frac{k_f}{M}x_3 \\ -\frac{k_e}{L}x_2 - \frac{R}{L}x_3 + \frac{1}{L}u \end{bmatrix} \tag{5}$$

where $F_{cm} = F_c + (F_m - F_c)\, e^{-\alpha\,|\dot{x}(t)|}$ and the state vector contains three quantities: position, speed and current:

$$\boldsymbol{x} = \begin{bmatrix} x_1 & x_2 & x_3 \end{bmatrix}^T = \begin{bmatrix} x & \dot{x} & i \end{bmatrix}^T. \tag{6}$$

3. Control problem solution

The method in its classic form is well described in [1, 10]. Interested readers can follow the state-dependent Riccati equation (SDRE) approach in the context of the nonlinear regulator problem [8–10].

The finite-time control problem consists of finding optimal control that minimizes the following objective function in finite time t_f [6]:

$$J(\boldsymbol{u}) = \frac{1}{2}\boldsymbol{x}^T(t_f)\boldsymbol{S}\,\boldsymbol{x}(t_f) + \frac{1}{2}\int_0^{t_f} \left(\boldsymbol{x}^T\boldsymbol{Q}\,\boldsymbol{x} + \boldsymbol{u}^T\boldsymbol{R}\,\boldsymbol{u}\right)\mathrm{d}t, \tag{7}$$

subject to nonlinear dynamics for affine systems:

$$\dot{\boldsymbol{x}} = \boldsymbol{F}(\boldsymbol{x}) + \boldsymbol{B}\,\boldsymbol{u}. \tag{8}$$

Nonlinear dynamics (2) can be rewritten in the form of the state-dependent coefficient (SDC) [12]:

$$\dot{\boldsymbol{x}} = \boldsymbol{A}(\boldsymbol{x})\boldsymbol{x} + \boldsymbol{B}\,\boldsymbol{u} \tag{9}$$

where $\boldsymbol{S}$ and $\boldsymbol{Q}$ are symmetric, positive semi-definite weighting matrices for states while $\boldsymbol{R}$ is the symmetric, positive definite weighting matrix for control inputs. The vector $\boldsymbol{F}(\boldsymbol{x})$ is piecewise continuous over time and smooth in respect of their arguments which satisfy the Lipschitz condition.

If the pair $\{\boldsymbol{A}(\boldsymbol{x}),\, \boldsymbol{B}\}$ constitutes stabilizable parameterization of the nonlinear system (9), then to check controllability of the affine system, this pair should be controllable in the linear sense.

Otherwise, checking controllability of that pair does not need the state or control input information [16]. It can be simply checked by a controllability matrix:

$$\boldsymbol{M}(\boldsymbol{x}) = \begin{bmatrix} \boldsymbol{B} & \boldsymbol{A}(\boldsymbol{x})\boldsymbol{B} & \ldots & \boldsymbol{A}^{n-1}(\boldsymbol{x})\boldsymbol{B} \end{bmatrix}. \tag{10}$$

The system is controllable if the controllability matrix has full rank.

In the proposed case, the fast controller is formulated as in the classic SDRE form (7)–(8), but SDC parametrized form of (8) uses a separated form of matrix $\boldsymbol{A}(\boldsymbol{x})$:

$$\dot{\boldsymbol{x}} = (\boldsymbol{A_1} + \boldsymbol{A_2}(\boldsymbol{x}))\boldsymbol{x} + \boldsymbol{B}\,\boldsymbol{u}. \tag{11}$$

As in the previous case, to check controllability of the affine system (11), the pair $\{\boldsymbol{A_1} + \boldsymbol{A_2}(\boldsymbol{x}),\, \boldsymbol{B}\}$ should be controllable. This means that the controllability matrix:

$$\boldsymbol{M}(\boldsymbol{x}) = \begin{bmatrix} \boldsymbol{B} & \boldsymbol{A_1}\boldsymbol{B} & \ldots & \boldsymbol{A_1^{n-1}}\boldsymbol{B} \end{bmatrix} \tag{12}$$

should have full rank.

Using the Hamiltonian theory:

$$H = \frac{1}{2}\left(\boldsymbol{x}^T\mathbf{Q}\mathbf{x} + \mathbf{u}^T\mathbf{R}\mathbf{u} + \boldsymbol{p}^T\left((\boldsymbol{A_1} + \boldsymbol{A_2}(\boldsymbol{x}))\boldsymbol{x} + \mathbf{B}\mathbf{u}\right)\right), \tag{13}$$

and considering the necessary optimality condition $\frac{\partial H}{\partial \boldsymbol{u}} = \boldsymbol{0}$ with $\boldsymbol{p} = (\boldsymbol{K_1} + \boldsymbol{K_2}(\boldsymbol{x}))\boldsymbol{x}$, results in the following control law:

$$\boldsymbol{u} = -\boldsymbol{R}^{-1}\boldsymbol{B}^T(\boldsymbol{K_1} + \boldsymbol{K_2}(\boldsymbol{x}))\boldsymbol{x}. \tag{14}$$

The control law (14) includes two feedback compensators. The first is constant and the second is state-dependent.

Employing the optimality condition, the nonlinear system is described by the following state-space equation:

$$\dot{\boldsymbol{x}} = (\boldsymbol{A_1} + \boldsymbol{A_2}(\boldsymbol{x}))\boldsymbol{x} - \boldsymbol{B}\boldsymbol{R}^{-1}\boldsymbol{B}^T\boldsymbol{p} \tag{15}$$

and the adjoining differential equation:

$$\dot{\boldsymbol{p}} = -\left(\boldsymbol{A_1} + \frac{\partial\left(\boldsymbol{A_2}(\boldsymbol{x})\boldsymbol{x}\right)}{\partial \boldsymbol{x}}\right)^T \boldsymbol{p} - \boldsymbol{Q}\,\boldsymbol{x}, \tag{16}$$

where:

$$\frac{\partial\left(\boldsymbol{A_2}(\boldsymbol{x})\boldsymbol{x}\right)}{\partial \boldsymbol{x}} = \boldsymbol{A_2}(\boldsymbol{x}) + \frac{\partial \boldsymbol{A_2}(\boldsymbol{x})}{\partial \boldsymbol{x}}\boldsymbol{x}. \tag{17}$$

Substituting $\boldsymbol{p} = (\boldsymbol{K_1} + \boldsymbol{K_2}(\boldsymbol{x}))\boldsymbol{x}$ into (16), the state-space nonlinear equation can be written as:

$$\dot{\boldsymbol{x}} = \left(\boldsymbol{A_1} - \boldsymbol{B}\boldsymbol{R}^{-1}\boldsymbol{B}^T\boldsymbol{K_1}\right)\boldsymbol{x} + \left(\boldsymbol{A_2}(\boldsymbol{x}) - \boldsymbol{B}\boldsymbol{R}^{-1}\boldsymbol{B}^T\boldsymbol{K_2}(\boldsymbol{x})\right)\boldsymbol{x}. \tag{18}$$

The first bracket of equation (18) is state-independent and the second one is state-dependent, thus there is a possibility to linearize it and solve the state-dependent gain matrix $\boldsymbol{K_2}(\boldsymbol{x})$:

$$\boldsymbol{K_2}(\boldsymbol{x}) = \left[\boldsymbol{B}\boldsymbol{R}^{-1}\boldsymbol{B}^T\right]^+\boldsymbol{A_2}(\boldsymbol{x}). \tag{19}$$

Matrix $\boldsymbol{B}\boldsymbol{R}^{-1}\boldsymbol{B}^T$ is singular, thus the state-dependent gain matrix $\boldsymbol{K_2}(\boldsymbol{x})$ may be computed only by means of the pseudoinverse operation. To perform the operation, a Moore-Penrose pseudoinverse is applied. The Moore-Penrose pseudoinverse is defined for such matrix and is unique [2].

Using differential equation (16) with $\boldsymbol{p} = (\boldsymbol{K_1} + \boldsymbol{K_2}(\boldsymbol{x}))\boldsymbol{x}$, the nonlinear differential optimal control equation (NDOCE) takes the form below:

$$\begin{aligned}
&\boldsymbol{A}_1^T\boldsymbol{K_1} + \boldsymbol{K_1}\boldsymbol{A_1} - \boldsymbol{K_1}\boldsymbol{B}\boldsymbol{R}^{-1}\boldsymbol{B}^T\boldsymbol{K_1} + \mathbf{Q} + \dot{\boldsymbol{K}}_1 + \dot{\boldsymbol{K}}_2(\boldsymbol{x}) + \\
&\quad + \left(\frac{\partial \boldsymbol{A_2}(\boldsymbol{x})}{\partial \boldsymbol{x}}\boldsymbol{x}\right)^T \boldsymbol{K_2}(\boldsymbol{x}) + \left(\frac{\partial \boldsymbol{A_2}(\boldsymbol{x})}{\partial \boldsymbol{x}}\boldsymbol{x}\right)^T \boldsymbol{K_1} + \\
&\quad + \boldsymbol{A}_2^T(\boldsymbol{x})\boldsymbol{K_1} + \boldsymbol{K_1}\boldsymbol{A_2}(\boldsymbol{x}) + \boldsymbol{A}_1^T\boldsymbol{K_2}(\boldsymbol{x}) + \boldsymbol{K_2}(\boldsymbol{x})\boldsymbol{A_1} + \\
&\quad + \boldsymbol{A}_2^T(\boldsymbol{x})\boldsymbol{K_2}(\boldsymbol{x}) + \boldsymbol{K_2}(\boldsymbol{x})\boldsymbol{A_2}(\boldsymbol{x}) + \\
&\quad + \boldsymbol{K_2}(\boldsymbol{x})\boldsymbol{B}\boldsymbol{R}^{-1}\boldsymbol{B}^T\boldsymbol{K_1} - \boldsymbol{K_1}\boldsymbol{B}\boldsymbol{R}^{-1}\boldsymbol{B}^T\boldsymbol{K_2}(\boldsymbol{x}) + \\
&\quad + \boldsymbol{K_2}(\boldsymbol{x})\boldsymbol{B}\boldsymbol{R}^{-1}\boldsymbol{B}^T\boldsymbol{K_2}(\boldsymbol{x}) = \mathbf{0}.
\end{aligned} \tag{20}$$

Based on linearization (18)–(19), it can be assumed that matrix $\boldsymbol{K_1}$ solves (20), considering its part called the differential Riccati equation (DRE) [13–15]

$$\dot{\boldsymbol{K}}_1 + \boldsymbol{A}_1^T\boldsymbol{K_1} + \boldsymbol{K_1}\boldsymbol{A_1} - \boldsymbol{K_1}\boldsymbol{B}\boldsymbol{R}^{-1}\boldsymbol{B}^T\boldsymbol{K_1} + \mathbf{Q} = \mathbf{0} \tag{21}$$

with the rest treated as the optimality condition:

$$\begin{aligned}
&\dot{\boldsymbol{K}}_2(\boldsymbol{x}) + \left(\frac{\partial \boldsymbol{A_2}(\boldsymbol{x})}{\partial \boldsymbol{x}}\boldsymbol{x}\right)^T \boldsymbol{K_2}(\boldsymbol{x}) + \left(\frac{\partial \boldsymbol{A_2}(\boldsymbol{x})}{\partial \boldsymbol{x}}\boldsymbol{x}\right)^T \boldsymbol{K_1} + \\
&\quad + \boldsymbol{A}_2^T(\boldsymbol{x})\boldsymbol{K_1} + \boldsymbol{K_1}\boldsymbol{A_2}(\boldsymbol{x}) + \boldsymbol{A}_1^T\boldsymbol{K_2}(\boldsymbol{x}) + \boldsymbol{K_2}(\boldsymbol{x})\boldsymbol{A_1} + \\
&\quad - \boldsymbol{K_2}(\boldsymbol{x})\boldsymbol{B}\boldsymbol{R}^{-1}\boldsymbol{B}^T\boldsymbol{K_1} - \boldsymbol{K_1}\boldsymbol{B}\boldsymbol{R}^{-1}\boldsymbol{B}^T\boldsymbol{K_2}(\boldsymbol{x}) + \\
&\quad + \boldsymbol{K_2}(\boldsymbol{x})\boldsymbol{B}\boldsymbol{R}^{-1}\boldsymbol{B}^T\boldsymbol{K_2}(\boldsymbol{x}) = \mathbf{0}
\end{aligned} \tag{22}$$

for $\boldsymbol{K_2}(\boldsymbol{x})$ obtained from (19).

It can be seen from the above that compensator separation represented by $\boldsymbol{K}(\boldsymbol{x}) = \boldsymbol{K_1} + \boldsymbol{K_2}(\boldsymbol{x})$ on the linear and nonlinear part makes it possible to solve the differential Riccati equation (DRE) for $\boldsymbol{K_1}$:

$$\dot{\boldsymbol{K}}_1 + \boldsymbol{A}_1^T\boldsymbol{K_1} + \boldsymbol{K_1}\boldsymbol{A_1} - \boldsymbol{K_1}\boldsymbol{B}\boldsymbol{R}^{-1}\boldsymbol{B}^T\boldsymbol{K_1} + \mathbf{Q} = \mathbf{0} \tag{23}$$

and $\boldsymbol{K_2}(\boldsymbol{x})$:

$$\boldsymbol{K_2}(\boldsymbol{x}) = \left[\boldsymbol{B}\boldsymbol{R}^{-1}\boldsymbol{B}^T\right]^+ \boldsymbol{A_2}(\boldsymbol{x}) \tag{24}$$

employing the Moore-Penrose pseudoinverse [2].

Equation (23) is state-independent and needs to be solved only once the control process is completed with final condition $\boldsymbol{K_1}(t_f) = \boldsymbol{S} - \left[\boldsymbol{B}\boldsymbol{R}^{-1}\boldsymbol{B}^T\right]^+ \boldsymbol{A_2}\left(\boldsymbol{x}(t_f)\right)$. So, in comparison to the classic SDRE approach, the computational effort is strongly reduced. Consequently, control law implementation becomes much easier in the real control system.

4. Stability proof

Asymptotic stability of the closed-loop system (18) implies that it is possible to control the states from the initial values to the final ones. However, the global stability property is difficult to prove [1, 4, 7, 17–20]. The controlled system with the SDRE compensator-based feedback is locally asymptotically stable.

The system (11) is such that $(\boldsymbol{A_1} + \boldsymbol{A_2}(\boldsymbol{x}))\mathbf{x}$ and $\dfrac{\partial\left(\boldsymbol{A_1}\boldsymbol{x} + \boldsymbol{A_2}(\boldsymbol{x})\boldsymbol{x}\right)}{\partial \boldsymbol{x}}$ are continuous in $\boldsymbol{x}$ for all $\|\boldsymbol{x}\| < r$, where $r > 0$ is the largest radius in some nonempty neighborhood of the original $\boldsymbol{x} = \mathbf{0}$. Assuming that the system is stabilizable at equilibrium point $\boldsymbol{x} = \mathbf{0}$, it is possible to define matrix $\boldsymbol{K_1}$ so that all eigenvalues of matrix $\left(\boldsymbol{A_1} - \boldsymbol{B}\boldsymbol{R}^{-1}\boldsymbol{B}^T\boldsymbol{K_1}\right)$ which describes the linear part of the closed-loop system, have negative real parts. For all eigenvalues of the matrix there exists any $\beta > 0$, such that $\operatorname{Re}\left(\boldsymbol{A_1} - \boldsymbol{B}\boldsymbol{R}^{-1}\boldsymbol{B}^T\boldsymbol{K_1}\right) < -\beta$.

Having the system:

$$\dot{\boldsymbol{x}} = \left(\boldsymbol{A_1} - \boldsymbol{B}\boldsymbol{R}^{-1}\boldsymbol{B}^T\boldsymbol{K_1}\right)\boldsymbol{x} + \left(\boldsymbol{A_2}(\boldsymbol{x}) - \boldsymbol{B}\boldsymbol{R}^{-1}\boldsymbol{B}^T\boldsymbol{K_2}(\mathbf{x})\right)\boldsymbol{x}. \tag{25}$$

Let:

$$g(\boldsymbol{x}) = \boldsymbol{A_2}(\boldsymbol{x}) - \boldsymbol{B}\boldsymbol{R}^{-1}\boldsymbol{B}^T\boldsymbol{K_2}(\boldsymbol{x}) \tag{26}$$

and $h(\boldsymbol{x}) = g(\boldsymbol{x})\boldsymbol{x}$, and then the system is:

$$\dot{\boldsymbol{x}} = \left(\boldsymbol{A_1} - \boldsymbol{B}\boldsymbol{R}^{-1}\boldsymbol{B}^T\boldsymbol{K_1}\right)\boldsymbol{x} + h(\boldsymbol{x}). \tag{27}$$

From (19) it becomes obvious that:

$$h(\boldsymbol{x}) \approx 0, \quad \text{because} \quad \lim_{\|\boldsymbol{x}\| \to 0} \frac{\|h(\boldsymbol{x})\|}{\|\boldsymbol{x}\|} = 0. \tag{28}$$

By the assumptions of $(\boldsymbol{A_1} + \boldsymbol{A_2}(\boldsymbol{x}))\boldsymbol{x}$, $\dfrac{\partial\left(\boldsymbol{A_1}\boldsymbol{x} + \boldsymbol{A_2}(\boldsymbol{x})\boldsymbol{x}\right)}{\partial \boldsymbol{x}}$ and by continuity, the solution (27) exists in the time interval $t \in [0, t_f]$ and takes the following form:

$$\boldsymbol{x}(t) = \mathrm{e}^{\left(\boldsymbol{A_1} - \boldsymbol{B}\boldsymbol{R}^{-1}\boldsymbol{B}^T\boldsymbol{K_1}\right)t}\boldsymbol{x}(0). \tag{29}$$

Taking the norm of the above solution:

$$\|\boldsymbol{x}(t)\| \le \left\|\mathrm{e}^{\left(\boldsymbol{A_1} - \mathbf{B}\boldsymbol{R}^{-1}\boldsymbol{B}^T\boldsymbol{K_1}\right)t}\right\| \|\boldsymbol{x}(0)\|, \tag{30}$$

hence $\|g(\boldsymbol{x})\| \to 0$ as $\|\boldsymbol{x}\| \to 0$ and $h(\boldsymbol{x})$ satisfies condition (30). From theoretical results on almost linear systems it is known that if the eigenvalues of $\left(\boldsymbol{A_1} - \boldsymbol{B}\boldsymbol{R}^{-1}\boldsymbol{B}^T\boldsymbol{K_1}\right)$ have negative real parts, $h(\boldsymbol{x})$ can be very small but continuous around the origin, and if condition (30) holds, then $\boldsymbol{x} = \mathbf{0}$ is asymptotically stable.

When providing the proof, let us consider solution (29) and let $\mu > 0$ be given. Then there exist a $\delta \in (0, r)$ such that $\|h(\boldsymbol{x})\| \le \mu\|\boldsymbol{x}\|$ whenever $\|\boldsymbol{x}\| \le \delta$, and consequently the solution to (29) can be expressed as:

$$\begin{aligned}
\boldsymbol{x}(t) = {} & \mathrm{e}^{\left(\boldsymbol{A_1} - \boldsymbol{B}\boldsymbol{R}^{-1}\boldsymbol{B}^T\boldsymbol{K_1}\right)t}\boldsymbol{x}(0) + \\
& + \int_0^t \mathrm{e}^{\left(\boldsymbol{A_1} - \boldsymbol{B}\boldsymbol{R}^{-1}\boldsymbol{B}^T\boldsymbol{K_1}\right)(t-s)} h(\boldsymbol{x}(s))\,\mathrm{d}s.
\end{aligned} \tag{31}$$

Taking the norm of both sides:

$$\begin{aligned}\|\boldsymbol{x}(t)\| \, & \left\| \mathrm{e}^{\left(\boldsymbol{A}_1 - \boldsymbol{B}\boldsymbol{R}^{-1}\boldsymbol{B}^T\boldsymbol{K}_1\right)t} \right\| \|\boldsymbol{x}(0)\| \\ & + \int_0^t \left\| \mathrm{e}^{\left(\boldsymbol{A}_1 - \boldsymbol{B}\boldsymbol{R}^{-1}\boldsymbol{B}^T\boldsymbol{K}_1\right)(t-s)} \right\| \|x(s)\| \, \mathrm{d}s, \end{aligned} \tag{32}$$

there exists a positive constant G such that:

$$\left\| \mathrm{e}^{\left(\boldsymbol{A}_1 - \boldsymbol{B}\boldsymbol{R}^{-1}\boldsymbol{B}^T\boldsymbol{K}_1\right)t} \right\| \leq G\mathrm{e}^{-\beta t} \tag{33}$$

which implies:

$$\|\boldsymbol{x}(t)\| \leq G\mathrm{e}^{-\beta t} \|\boldsymbol{x}(0)\| + \mu G \int_0^t \mathrm{e}^{-\beta(t-s)} \|x(s)\| \, \mathrm{d}s. \tag{34}$$

Invoking Grönwall's inequality and multiplying by $\mathrm{e}^{\beta t}$

$$\|\boldsymbol{x}(t)\| \leq G \|\boldsymbol{x}(0)\| \, \mathrm{e}^{-(\beta - \mu G)t}, \tag{35}$$

since $\beta - \mu G > 0$, then $\boldsymbol{x} = \boldsymbol{0}$ is indeed asymptotically stable.

5. Linear actuator control

The linear actuator model is applied to check the described finite-time SDRE control. Governing equations that describe actuator dynamics are given by (5).

At first, the linear actuator step response behavior (open-loop system) is considered when constant pin voltage $u = -24$ V is applied with stroke initial position $x_1 = 0.1$ m. The actuator model parameters are presented in Table 1.

Table 1
Actuator model parameters.

Parameter	Value [quantity]
M	0.25 [kg]
k_f	0.02 [kgm/s^{2}A]
F_c	0.005 [kg/s]
F_m	0.01 [kg/s]
α	2
β	1.4 [kg/s]
R	9.75 [Ω]
L	2.4 [mH]
k_e	0.75 [Vs/m]

Simulations are compared to measurement.

Next, the proposed SDRE method is applied to control the electric linear actuator for three finite times: $t_f = 2$ s, $t_f = 2.5$ s and $t_f = 3$ s. As mentioned in the introduction, the time is very important, because the actuator controls the spreading angle of the spreading device. The angle must sometimes be changed rapidly to avoid approaching vehicles or other objects during spreading action.

The problem consists in finding state dynamics and SDRE control. In association with actuator dynamics (5), the quadratic cost functional weighting matrices in (7) are chosen as $\mathbf{S} = \begin{bmatrix} 0.1 & 0 & 10 \\ 0 & 0 & 0 \\ 10 & 0 & 0 \end{bmatrix}$, $\mathbf{Q} = diag\,(0,\ \beta,\ R)$ and $\boldsymbol{R} = 1/R$ with initial conditions for stroke position $x = 0.1m$ and motor current $i = 2.5$ A, while on the other hand $x_0 = \begin{bmatrix} 0.1 & 0 & 2.5 \end{bmatrix}^T$.

Fig. 4–6 show open-loop voltage control applied to the linear actuator and step responses used in order to verify the model and confirm that the nonlinear model is useful for checking and formulating a new SDRE control method.

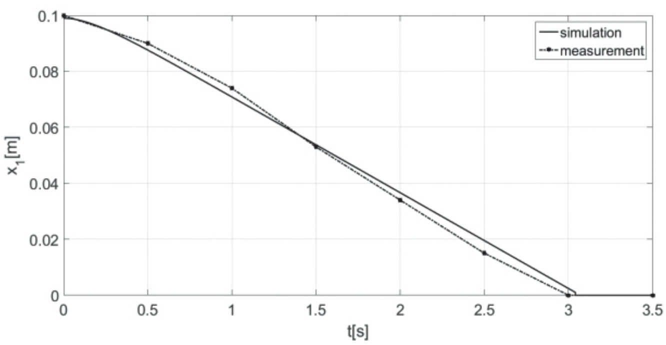

Fig. 4. Simulated and measured step response of stroke position.

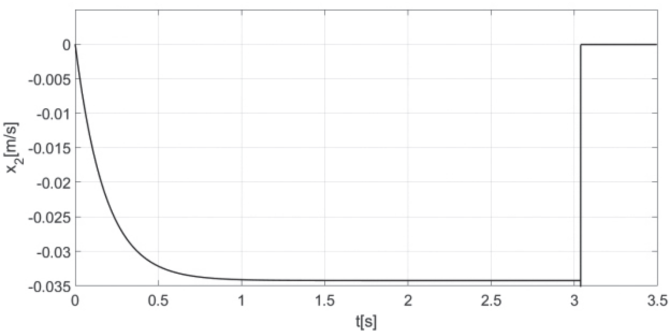

Fig. 5. Simulated step response of stroke speed.

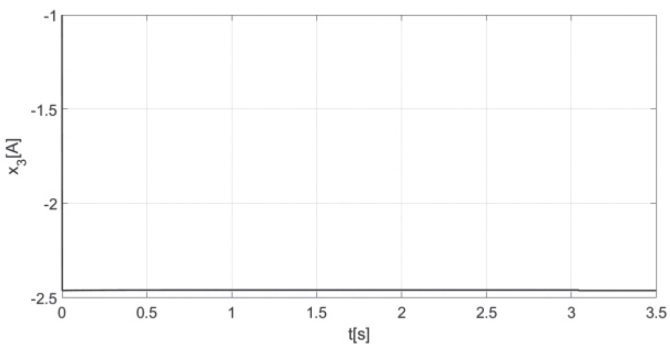

Fig. 6. Simulated step response of actuator current.

Fig. 7–10 show that for the assumed initial condition, the actuation system can be positioned from initial to final position in the prescribed time. Moreover, the stroke positioning is organized performing soft-start and soft-end tasks (Fig. 7).

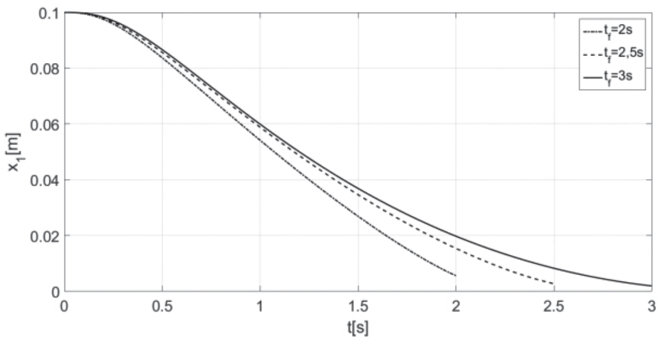

Fig. 7. Stroke positions.

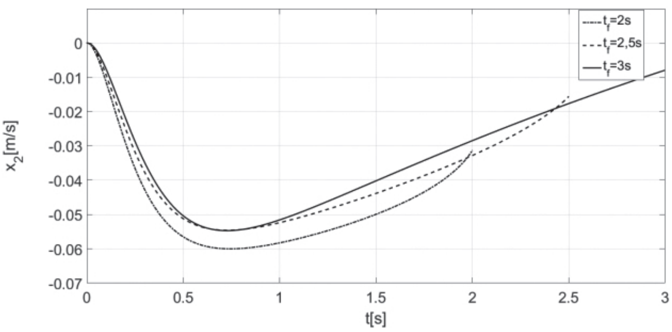

Fig. 8. Stroke speeds.

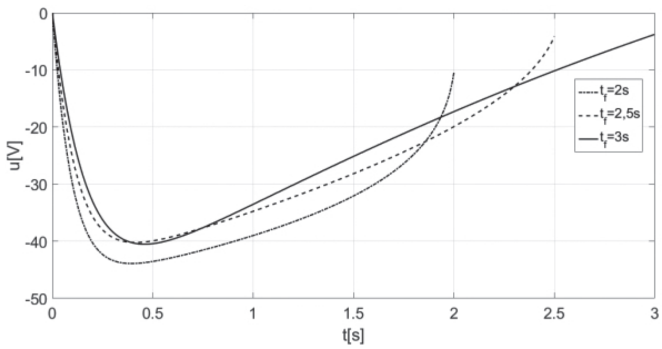

Fig. 9. SDRE controls.

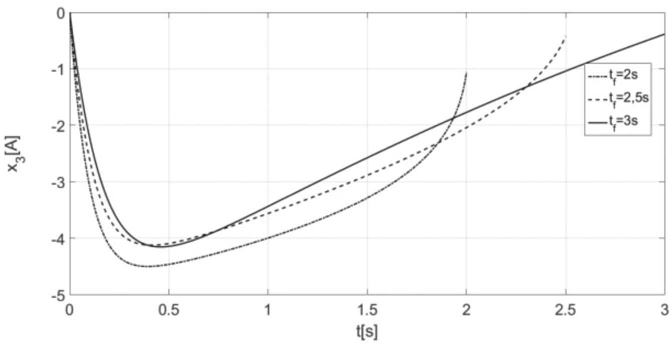

Fig. 10. Actuator currents.

Control time reduction is related to increasing the amplitude of the applied actuator voltage and current. Also, the advantage of the presented method is that the electric actuator can be controlled minimizing energy delivered and energy lost in the spreading control system.

Control of the width of the spreading pattern in a finite-time set-up has a huge practical impact. As mentioned in the introduction section, this function is important when the spreading pattern width must be changed rapidly to avoid approaching vehicles or other objects during spreading action, because sometimes fractions of seconds are important when cars or other vehicles move at high speed.

6. Conclusions

The finite time control problem for the linear actuator as a plant of high-performance and optimal drive system for spreading devices systems with a nonlinear feedback compensator is formulated and solved herein. The method for computation of suboptimal control input minimizes energy delivered to the spreading control system and energy lost, performing the soft-start and soft-end task. The effectiveness of the technique presented is demonstrated on a numerical example where optimal voltage control is found for different final times.

References

[1] H.T. Banks, B.M. Lewis, and H.T. Tran, "Nonlinear feedback controllers and compensators: a state-dependent Riccati equation approach", *Comput. Optim. Appl* 37, 177–218 (2007).

[2] J.C.A. Barata and M.S. Hussein, *The Moore-Penrose Pseudoinverse. A Tutorial Review of the Theory*, John Hopkins University Press (2013).

[3] N. Wang, J. Yu, and W. Lin, *Positioning control of linear actuator with nonlinear friction and input saturation using output feedback control*, Wiley Periodicals Inc. 21(S2), 191–200 (2016).

[4] K.K. Varanasi and S. Nayfeh, "The dynamics of leadscrew drivers: low order modeling and experiments", *Transactions of ASME* 126, 388–396 (2004).

[5] S.E. Lyshevski, *Electromechanical Systems, Electric Machines, and Applied Mechatronics*, CRC Press (1999).

[6] A. Wernli and G. Cook, "Suboptimal control for the nonlinear quadratic regulator problem", *Automatica* 11, 75–84 (1975).

[7] E.B. Erdem and A.G. Alleyne, "Globally stabilizing second-order nonlinear systems by SDRE control", In: *Proceedings of the American Control Conference*, San Diego, CA. IEEE, Los Alamitos (1999).

[8] C.P. Mracek and J.R. Cloutier, "Control designs for the nonlinear benchmark problem via the state-dependent Riccati equation method", *Int. J. Robust Nonlinear Control* 8 (4–5), 401–433 (1998).

[9] T. Cimen and S.P. Banks, "Global optimal feedback control for general nonlinear systems with non-quadratic performance criteria", *Syst. Control Lett* 53, 327–346 (2004).

[10] T. Cimen and S.P. Banks, "Nonlinear optimal tracking control with application to super-tankers for autopilot design", *Automatica* 40, 1845–1863 (2004).

[11] J.D. Pearson, "Approximation methods in optimal control", *Journal of Electronics and Control* 13, 453–469 (1962).

[12] Y.-W. Liang and L.-G. Lin, "Analysis of SDC matrices for successfully implementing the SDRE scheme", *Automatica* 49, 3120–3124 (2013).

[13] A. Bracci, M. Innocenti, and L. Pollini, "Estimation of the region of attraction for state-dependent Riccati equation controllers", *Journal of Guidance, Control and Dynamics* 29 (6), 1427–1430 (2006).

[14] T. Çimen, "Systematic and effective design of nonlinear feedback controllers via the state-dependent Riccati equation (SDRE) method", *Annual Reviews in Control* 34(1), 32–51 (2010).

[15] E.B. Erdem and A.G. Alleyne, "Design of a class of nonlinear controllers via state dependent Riccati equations", *IEEE Transactions on Control Systems Technology* 12(1), 133–137 (2004).

[16] K.D. Hammett, C.D. Hall, and D.B. Ridgely, "Controllability issues in nonlinear state-dependent Riccati equation control", *Journal of Guidance, Control and Dynamics* 21 (5), 767–773 (1998).

[17] Q.M. Lam, M. Xin, and J.R. Cloutier, "SDRE control stability criteria and convergence issues: where are we today addressing practitioners' concerns?" In AIAA paper, 2012–2475 (2012).

[18] Y.-W. Liang and L.-G. Lin, "On factorization of the nonlinear drift term for SDRE approach", In *Proc. of the 18th world congress IFAC*, Milano, Italy, 9607–9612 (2011).

[19] J.S. Shamma and J.R. Cloutier, "Existence of SDRE stabilizing feedback", *IEEE Transactions on Automatic Control* 48 (3), 513–517 (2003)

[20] M. Sznaier, J. Cloutier, R. Hull, D. Jacques, and C. Mracek, "Receding horizon control Lyapunov function approach to suboptimal regulation of nonlinear systems", *Journal of Guidance, Control and Dynamics* 23 (3), 399–405 (2000).

[21] M. Siwczynski and K. Hawron, "Optimum tasks and solutions for energy transmission from the source to the receiver", *Bull. Pol. Ac.: Tech.* 66(5), 655–663 (2018).

[22] www.dobrowolski.com.pl